ACS Pharmacology & Translational Science

pubs.acs.org/ptsci

Article

A Primary Cell and Organoid Platform for Evaluating Pharmacological Responses in Mammary Epithelial Cells

Teneale A. Stewart* and Felicity M. Davis*

Cite This: *ACS Pharmacol. Transl. Sci.* 2020, 3, 63−75

Read Online

ACCESS | Metrics & More | Article Recommendations | Supporting Information

ABSTRACT: An essential process in predicting the *in vivo* pharmacological activity of a candidate molecule involves the evaluation of target responses using established model systems. While these models largely comprise immortalized cells, which are often serially passaged as monolayers on uniformly stiff substrates and are modified to overexpress one or more components of the pathway-of-interest, the importance of cell identity, heterogeneity, and three-dimensional (3D) context to target response is gaining increasing attention. Here, we assess intracellular calcium responses in mouse mammary epithelial cells in three distinct model systems: 3D primary organoids, 2D primary epithelial cells, and 2D immortalized cells. Specifically, we assess intracellular calcium responses to a number of extracellular signals implicated in the regulation of basal (or myoepithelial) cell function. These findings provide further insights into cell type and context-specific pharmacological responses in mammary epithelial cells and highlight the opportunities and challenges in the adoption of architecturally complex and heterogeneous *in vitro* assays in pharmacological research.

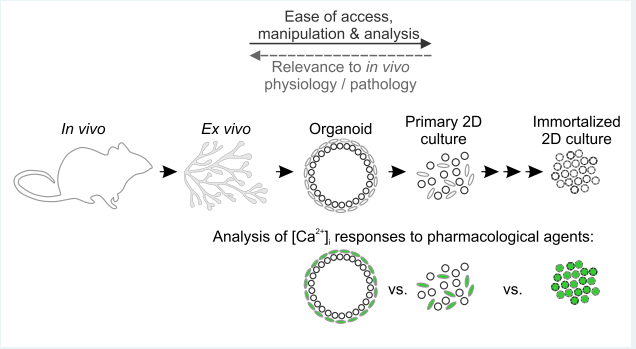

KEYWORDS: *organoids, mammary epithelial cells, calcium signaling, GCaMP6, adenosine 5′-triphosphate, oxytocin*

Essential to the process of drug discovery is understanding the way in which model systems respond to target (e.g., receptor and channel) modulation. Typically, these model systems take the form of two-dimensionally (2D) cultured, serially passaged cell lines, which are assumed to adequately reflect the behavior of cells within the tissue from which they were originally derived. While convenient (e.g., in terms of cost, labor, accessibility, and adaptability to high throughput screening methods), there are increasing concerns regarding the ability of immortalized cell lines to accurately predict drug responses *in vivo*. 2D immortalized cell culture models not only frequently differ in their phenotypic characteristics relative to their *in vivo* counterparts[1] but also have a lack of cell−cell and cell−extracellular-matrix interactions which further complicates the interpretation of responses to various stimuli *in vitro*.[2] In the case of mammary epithelial cells, the influence of 3D cellular architecture on stimulus response has been appreciated for some time.[3,4] Currently, the ability to monitor cell response and signal transduction processes downstream of target stimulation in real-time and *in situ* is limited to a few model organisms and activity readouts and is generally associated with high costs and low throughput.[5,6] Realizing the limitations associated with 2D cell culture systems and *in vivo* imaging, there has been increasing interest in moving toward the use of 3D organoids as a more physiologically relevant model for assessing cellular responses *in vitro* [recently reviewed in refs 7 and 8]. Unlike many immortalized cell-line-based 3D culture models, primary cell derived organoid cultures can maintain some of the cellular heterogeneity observed in the tissue of origin, including the presence of stem/progenitor and differentiated cell types. Oxygen and nutrient availability in these models is also easier to control compared to alternative 3D approaches (e.g., explant culture). Moreover, when grown in the presence of specialized growth factor cocktails, long-term culture can be achieved, a feature that is being leveraged for the creation of organoid "biobanks" for applications in disease modeling and drug screening.[9−11]

Intracellular calcium mobilization is a useful readout for measuring real-time cellular responses to target stimulation and is often employed as a surrogate for pharmacological activity *in vitro*, for example, small-molecule-mediated modulation of G protein-coupled receptor (GPCR) activity.[12,13] Typically, *in vitro* intracellular calcium readouts are based on fluorescent signals measured in cells loaded with synthetic dyes, such as Fura-2 (ratiometric) and Fluo-4 (nonratiometric).[14] While convenient to use and amenable to ratiometric imaging, experimental artifacts due to dye sequestration or uneven/

Special Issue: Emerging Leaders in Pharmacology and Translational Science

Received: October 30, 2019
Published: January 15, 2020

poor loading are not uncommon, and (owing to their eventual efflux) small molecule fluorescent indicators are not suited to long-term (>30−60 min) imaging. More recently, researchers have started turning to genetically encoded calcium indicators (GECIs), improved through multiple rounds of structure-guided design, as a tool to measure intracellular calcium responses, and their utility in high-throughput drug discovery is now being evaluated.[15,16] Unlike synthetic dye indicators, GECIs are incorporated into the host cell genome using standard molecular biology techniques, allowing for lineage-restricted expression and enabling imaging over periods of hours to days.[16] Advances in GECI targeting and live imaging platforms are also enabling visualization of calcium responses at subcellular resolution, including subplasma membrane domains and endoplasmic reticulum (ER) calcium responses,[17] providing greater spatiotemporal information in the engagement of this highly context-dependent signal transduction system.

The aim of this study was to determine the utility of activity imaging of agonist responses in dimensionally and biologically complex systems for pharmacological assays. This was achieved by comparing calcium signaling responses of mammary epithelial cells to physiologically relevant agonists using three distinct *in vitro* models—2D primary cell culture, 3D (organoid) primary cell culture, and 2D immortalized cell culture—in order to assess the contribution of cell identity and context to stimulus response. We show that primary 2D cultured cells and 3D organoids display similar calcium responses to different stimuli, which is distinct from those observed in immortalized mammary epithelial cells. Our findings support the hypothesis that cell identity, history, and context play an important role in receptor activation and may be more useful in understanding cellular responses to endogenous and exogenous agonists. Increased heterogeneity and dimensionality, however, provide additional challenges in analyzing and interpreting these data. Nevertheless, the increasing adoption of primary culture and organoid models, their combination with activity probes (e.g., calcium and voltage) and continued advances in imaging and image analysis, will undoubtedly spur further interest in these models as additional tools for drug discovery pursuits within both academia and industry, particularly those studies seeking to assess drug response and toxicity in breast cancer, which is also highly context-dependent.

RESULTS AND DISCUSSION

Mammary Epithelial Architecture Is Absent in 2D Primary and Immortalized Cell Culture. The mammary epithelium is a dynamic and plastic structure, which plays an important role in mammalian offspring survival.[18−21] Encircling a hollow lumen, which acts as a conduit for the passage of milk during lactation, is a well-defined epithelial bilayer, comprising an inner luminal cell layer and an outer basal cell layer, supported by a basement membrane (Figure 1A and Movie S1). Epithelial cell behaviors in this branching ductal network are guided by a range of extracellular factors, including diffusive cues, paracrine/juxtacrine signals, and physical interactions with both neighboring cells and the extracellular matrix.[19]

Primary cells cultured for short periods of time on 2D substrates retain cell lineage characteristics that are often altered or absent in immortalized, serially passaged cell lines.[1] Here, we show that lineage identity is retained in short-term (overnight) culture of primary mammary epithelial cells, as indicated by the presence of distinct cytokeratin (K)8$^+$ (luminal) and K5$^+$ (basal) epithelial cell populations, as observed *in vivo*[22,23] (Figure 1B).

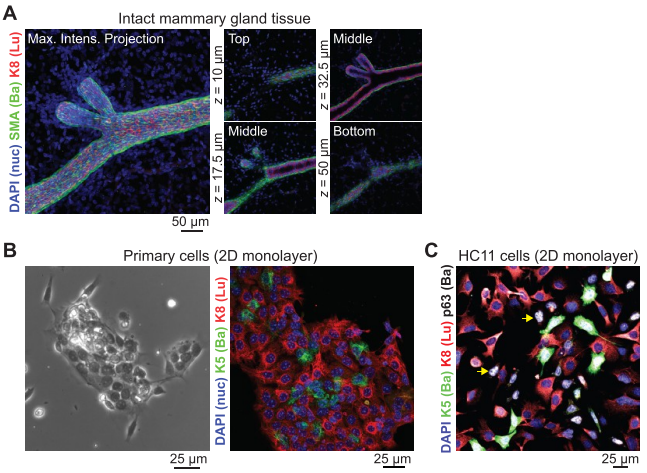

Figure 1. Structural complexity of mammary gland tissue is absent in 2D monolayer culture. (A) 3D maximum intensity projection of optically clear intact mammary gland tissue showing SMA$^+$ (green) basal epithelial cells and K8$^+$ (red) luminal epithelial cells. Nuclei are stained with DAPI (blue). The indicated depth (z) is relative to the first image acquired in the image series. Representative image from n = 3 mice. (B) Phase contrast (left) and confocal immunofluorescence (right) images of primary mammary epithelial cells grown in 2D monolayer culture. K5$^+$ (green) basal and K8$^+$ (red) luminal epithelial cell populations are observed. Nuclei are stained with DAPI (blue). Representative images of cells from n = 3 mice. (C) Confocal immunofluorescence image of 2D mouse mammary HC11 cells showing expression of luminal (K8, red) and basal (K5, green and p63, gray) markers. Yellow arrows indicate cells that are K8$^{+/lo}$, K5$^-$ and nuclear p63$^+$. Nuclei are stained with DAPI (blue). Images are representative of n = 3 independent experiments.

In monolayer-cultured HC11 immortalized mouse mammary epithelial cells, however, in addition to distinct K8$^+$ and K5$^+$ populations, 14 ± 3.7% were K8$^{+/lo}$, K5$^-$ and showed nuclear reactivity to the basal marker p63 (Figure 1C). The presence of dual-labeled K8$^{+/lo}$ and p63$^+$ cells may represent a characteristic potentially related to the reported "stem-like" capacity of this cell line[24] or, more likely, this may be a consequence of phenotypic alterations commonly observed in immortalized, serially cultured cell lines.[1] As expected, 2D cell culture methods suffer from a complete loss of cellular architecture and tissue context (Figure 1A versus 1B,C). Loss of architecture may be associated with altered signal transduction and cellular dynamics, including proliferation,[25,26] metabolic activity,[2] and drug response.[2,3,27] The impact of culture conditions on cellular signaling and drug handling is of particular relevance in early drug development and discovery, which has traditionally relied on 2D cell culture models, prompting a search for more physiologically relevant systems.[28−30]

3D Mammary Organoids Recapitulate the Organizational Complexity of the Ductal Epithelium *in Vitro*. An appreciation of the importance of cell−cell and cell−extracellular-matrix interactions in epithelial biology has led to the development of sophisticated 3D cell culture systems, which more closely recapitulate the complexity of organ systems *in vivo*.[29,31] Tissue-derived organoids represent one such model that is increasingly used to study epithelial cell biology and disease[9] and more recently in drug discovery.[28] Using a previously described protocol,[32] we created mammary organoids that exhibit an inner luminal K8$^+$ cell layer and an outer basal K5$^+$ cell layer, surrounding a hollow lumen (Figure 2A). However, in some organoids, regions comprising discontinuous

https://dx.doi.org/10.1021/acsptsci.9b00090
ACS Pharmacol. Transl. Sci. 2020, 3, 63−75

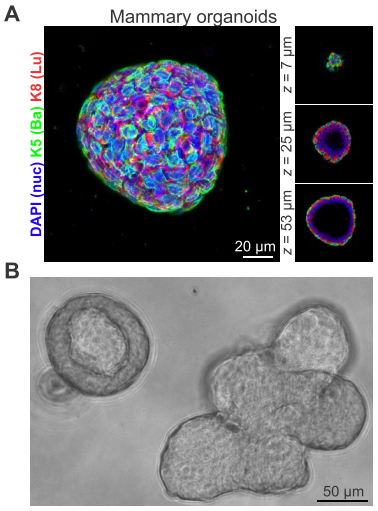

Figure 2. Mammary organoids maintain a physiologically relevant epithelial cell bilayer *in vitro*. (A) Confocal immunofluorescence images of mammary organoids grown for up to 21 days in culture. $K5^+$ (green) basal epithelial cells and $K8^+$ (red) luminal epithelial cells form a distinct bilayer surrounding a central lumen in mammary organoids grown *in vitro*. Nuclei are stained with DAPI (blue). The indicated depth (z) is relative to the first image acquired in the image series. (B) Phase contrast images of mammary organoids. Images are representative of organoids from $n = 3$ mice.

and/or multiple layers of cells were observed (Figure S1). Although this represents a departure from the *in vivo* ductal architecture, multiple luminal cell layers have been observed in other mammary organoid culture protocols, where they have been suggested to mimic the body region of terminal end buds.[33] We also observed heterogeneous budding structures in some organoids, as previously reported[32] (Figure 2B). Both of these features were more frequently seen with prolonged periods in culture (≥14 days). For the purposes of this focused study, we compare the utility and relevance of 2D and 3D short-term mammary culture models for real-time imaging in pharmacology research.

Development of a Genetically Engineered Mouse Model for Lineage-Specific Assessment of Intracellular Calcium Signaling *in Vitro*. The calcium ion is an important second messenger that plays a role in a number of signaling pathways relevant to drug discovery research. Increases in intracellular calcium can occur in mammary epithelial cells, for example, downstream of activation of certain G-protein coupled receptors [e.g., the oxytocin (OT) receptor],[6] tyrosine kinase receptors [e.g., the epidermal growth factor (EGF) receptor],[34] and ligand-gated ion channels [e.g., P2X receptors].[34] Assessment of intracellular calcium responses using synthetic dyes (e.g., Fura-2 and Fluo-4) or genetically encoded calcium indicators (e.g., GCaMP6f) can therefore offer a rapid, reliable, and proportional readout for receptor activation in pharmacology studies.[35]

Recently, OT-stimulated calcium oscillations were visualized in basal epithelial cells and linked to cell contraction and milk ejection in *ex vivo* mammary tissue harvested from lactating *GCaMP6f;K5CreERT2* mice.[6] In this model, tamoxifen administration induces the selective expression of GCaMP6f in >95% of basal cells[6] (Figure 3A), where it is capable of detecting increases in intracellular calcium with high sensitivity and fast kinetics.[6,36] Although valuable for mapping signal-response relationships at the tissue level, these *ex vivo* "explant" studies are laborious, expensive, and technically challenging, limiting their scope for medium- to high-throughput drug screening.

Using optically cleared mammary tissue from *GCaMP6f;K5-CreERT2* mice and an anti-GFP antibody that recognizes GCaMP6f, expression and lineage specificity of GCaMP6f was confirmed in smooth muscle actin $(SMA)^+$, $K8^-$ basal epithelial cells from nonpregnant (virgin) mice (Figure 3B), as previously characterized.[6] We also confirmed that GCaMP6f expression was primarily restricted to basal cells in dissociated mammary epithelial cells in primary 2D culture (Figure 3C) and in 3D organoid culture (Figure 3D). A small fraction of $GCaMP6f^+$ cells that were $p63^-$ or $K5^-$ were observed in primary 2D cell culture (Figures 3C and S2). As we did not detect any ambiguously or promiscuously labeled $GCaMP6f^+$ cells *in situ* or in 3D organoid studies, we hypothesize that a minor fraction of primary cells cultured overnight on a 2D substrate dedifferentiate, a well-recognized limitation associated with *in vitro* 2D culture of cell types that are highly dependent on microenvironmental signaling.[26,37,38] Having established expression of GCaMP6f in primary basal cells and basal cells in 3D organoids, we next assessed calcium signaling dynamics in these distinct systems to determine whether agonist responses differ in 2D versus 3D systems, as reported for other cell signaling events.[2,39]

Basal Mammary Epithelial Cell Calcium Responses Are Similar in 3D versus 2D Primary Cells but Not Immortalized Cells. As mentioned, ligand-induced cytosolic calcium increases provide a useful readout for assessing cellular responses to exogenous stimuli and represent a method frequently employed in pharmacology research.[14] Such studies are largely performed using immortalized, serially passaged, monolayer cell cultures loaded with cell permeant calcium dyes. Using cells derived from *GCaMP6f;K5CreERT2* mouse mammary tissue (Figure 3A), we were able to compare calcium responses of basal epithelial cells in both 2D and 3D culture, without the need of exogenously applied calcium sensitive dyes. To do this, we selected three physiologically relevant but distinct ligands: OT, adenosine 5′-triphosphate (ATP), and the wingless-type MMTV integration site family member 5a (Wnt5a). OT has a well-established role in regulating basal epithelial function in the functionally mature mammary gland, where it acts on the OT receptor, a GPCR that signals via intracellular calcium release, leading to a contractile response that is essential for milk expulsion in lactation.[6,40] The extracellular purine nucleotide ATP is recognized for its role in neurotransmission and secretory processes, but it is now also known to contribute to various pathologies, including inflammation[41] and tumor progression.[42] ATP-mediated cytosolic calcium increases occur downstream of purinergic receptor activation, which includes members of the P2X ionotropic and P2Y metabotropic families.[41] Similar to OT, ATP has been shown to act directly upon myoepithelial cells, including those in the lacrimal and mammary gland, eliciting a measurable calcium response.[43,44] WNT ligands play important roles in mammary gland development and include the noncanonical WNT ligand, Wnt5a, which is implicated in the regulation of stem/progenitor activity and ductal epithelial growth and side branching.[45,46] While calcium has been shown to transduce Wnt5a signaling events in other cell types,[47−49] less is known about the pathways by which this ligand mediates its effects in mammary epithelial cells. Recently, the receptor tyrosine kinase-like orphan receptor 2 (ROR2) and receptor-like tyrosine kinase (RYK) were identified as likely candidates;[46,50]

https://dx.doi.org/10.1021/acsptsci.9b00090
ACS Pharmacol. Transl. Sci. 2020, 3, 63−75

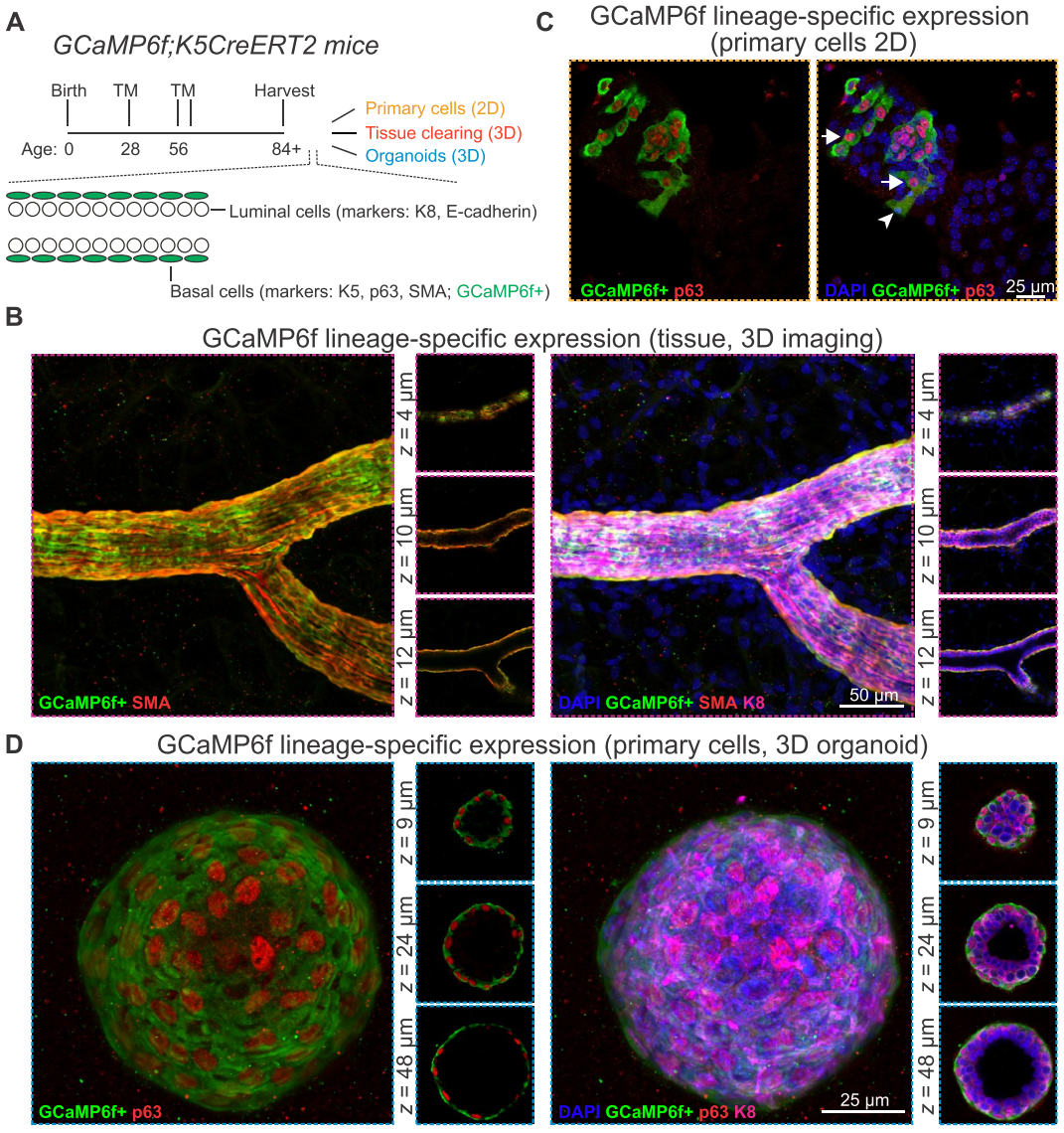

Figure 3. *In vitro* model for the lineage-specific assessment of calcium-dependent signal transduction. (A) Schematic representation of the induction schedule for the conditional *GCaMP6f;K5CreERT2* knock-in mouse model. (B) 3D maximum intensity projection of optically cleared mammary gland tissue showing lineage-specific expression of GCaMP6f (green) in SMA$^+$ (red) basal epithelial cells (left). GCaMP6f$^+$ cells (green) are distinct from K8 expressing (magenta) luminal epithelial cells (right). Nuclei are stained with DAPI (blue). The indicated depth (z) is relative to the first image acquired in the image series; $n = 2$ mice. (C) Confocal immunofluorescence images of 2D primary cells showing lineage-specific expression of GCaMP6f (green) in nuclear p63$^+$ (red) basal epithelial cells. White arrows indicate GCaMP6f$^+$, p63$^+$ cells. The arrow head indicates a GCaMP6f$^+$, p63$^-$ cell. Images are representative of $n = 3$ mice. (D) 3D maximum intensity projection of *GCaMP6f;K5CreERT2* mammary organoid showing the GCaMP6f$^+$ (green), p63$^+$ (red) outer basal epithelial cell layer (left) surrounding an inner K8$^+$ (magenta) luminal epithelial cell layer (right). Nuclei are stained with DAPI (blue). The indicated depth (z) is relative to the first image acquired in the image series. Images are representative of $n = 3$ mice.

calcium activation downstream of these pathways in 2D or 3D mammary epithelial cell cultures, however, remains entirely unexplored.

It is a well-appreciated phenomenon that when cultured on stiff 2D substrates primary cells may undergo a process of dedifferentiation resulting in phenotypic changes.[26,37] For this reason, we performed all calcium studies on 2D primary cells within 24 h of dissection (Figure 4A–E). Under these conditions, we observed heterogeneous (amplitude and frequency) calcium responses[6,51] in GCaMP6f$^+$ cells following addition of OT. This response was characterized by an initial large and transient rise in intracellular calcium ($[Ca^{2+}]_i$) in nearly all cells followed by subsequent, typically smaller calcium oscillations (Figures 4A and S3; Movie S2). These observations were confirmed using the automated calcium signal spike analysis tool, CaSiAn[52] (see the Methods and Figure 4E). Similarly, ATP stimulation produced a large initial calcium transient, which may involve activation of both P2X-mediated extracellular calcium influx as well as P2Y-mediated intracellular calcium release[53] (Figures 4B,E and S3; Movie S3). Publically available RNA sequencing data suggests that a number of P2X and P2Y receptors are expressed in basal epithelial cells from virgin mouse mammary gland,[54] and we confirmed in our laboratory that *P2rx1*, *P2rx4*, *P2rx5*, *P2ry1*, *P2ry2*, and *P2ry6* are expressed in mouse mammary tissue, via quantitative RT-PCR (Figure S4A). Both the initial and subsequent calcium responses of 2D primary cells to Wnt5a were of lower amplitude compared to those seen following treatment with OT and ATP, with

https://dx.doi.org/10.1021/acsptsci.9b00090
ACS Pharmacol. Transl. Sci. 2020, 3, 63–75

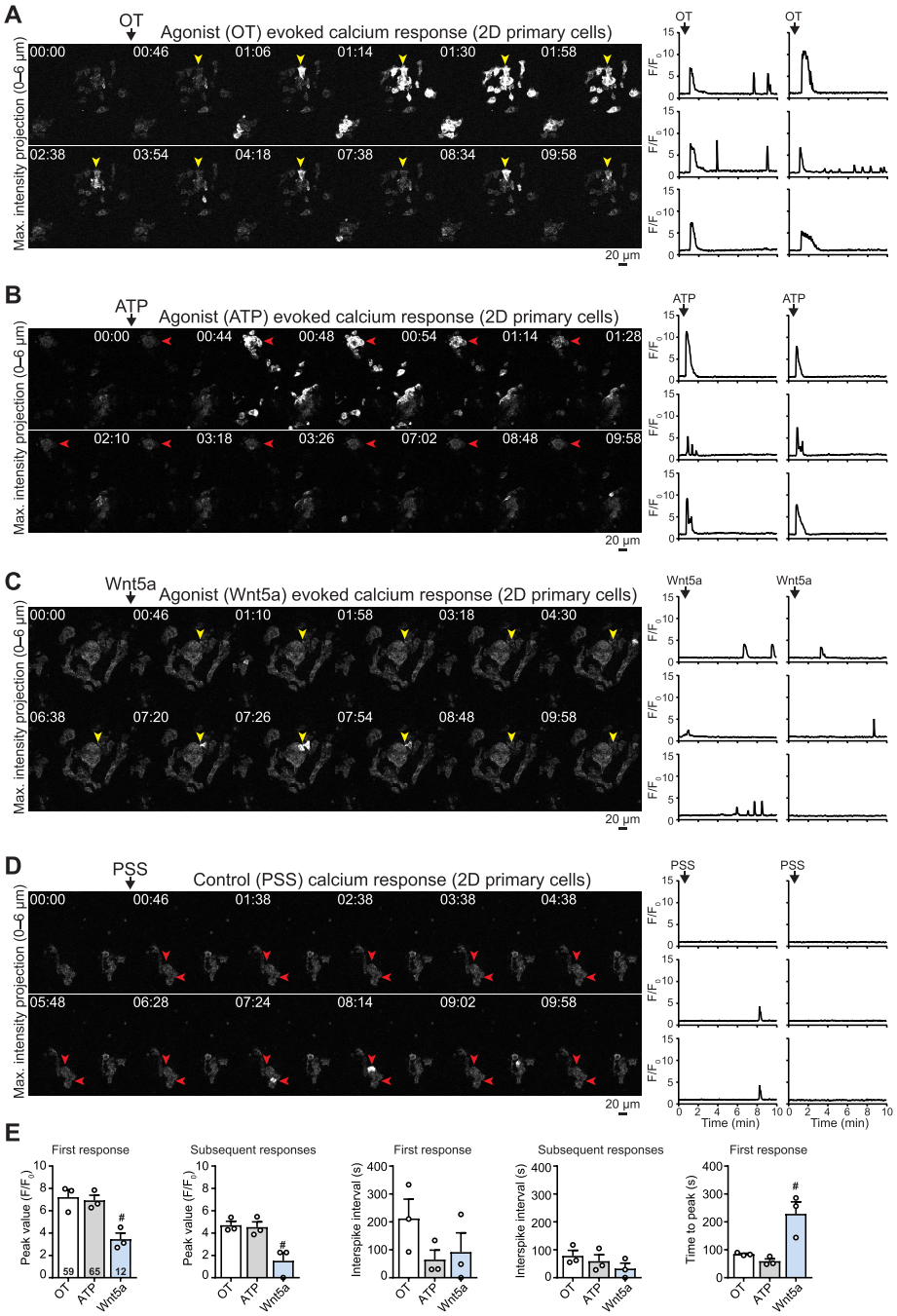

Figure 4. Lineage-specific assessment of calcium signaling in mammary primary epithelial cells cultured in 2D. Maximum intensity projection showing global cell calcium response (gray; left), and representative single cell calcium traces showing relative change in fluorescence intensity normalized to baseline (F/F_0) (right) from *GCaMP6f;K5CreERT2* 2D primary cells following stimulation with (A) OT, (B) ATP, (C) Wnt5a, and (D) PSS. Yellow arrows indicate cells that demonstrate repetitive calcium oscillations (≥2 per imaging series). Red arrows indicate cells that demonstrate a single calcium response. Representative of movies from $n = 3$ animals. (E) Quantitative analysis of calcium responses to agonist stimulation including, peak amplitude (peak value (F/F_0) of initial and secondary calcium spikes), time between consecutive calcium spikes (interspike interval (s)) and time to first calcium peak (s). Numbers denoted in bars indicate the number of cells (out of a total of 75) identified as responding to the corresponding agonist. Graphs show mean ± S.E.M., $n = 3$ independent experiments; #, $P < 0.05$ in OT and ATP relative to Wnt5a-stimulated primary cells, one-way ANOVA with Bonferroni post-tests.

typically only a small number of cells showing delayed transient responses (either single or oscillatory; Figures 4C,E and S3; Movie S4). These results may correlate with this agonist potentially acting on a less abundant population of mammary stem/progenitor cells.[46] Calcium responses following the addition of physiological salt solution (PSS; buffer) appeared to be less frequent and of lower amplitude and duration relative to the responses of the other ligands that were assessed in 2D primary cells (Figures 4D and S3; Movie S5).

Next, we analyzed agonist-evoked calcium signals in 3D organoids (Figure 5A–E). Consistent with the calcium response observed in 2D primary cells, 3D cultured GCaMP6f$^+$ cells exhibited an initial large and transient rise in $[Ca^{2+}]_i$ followed by smaller calcium oscillations in response to OT stimulation

https://dx.doi.org/10.1021/acsptsci.9b00090
ACS Pharmacol. Transl. Sci. 2020, 3, 63–75

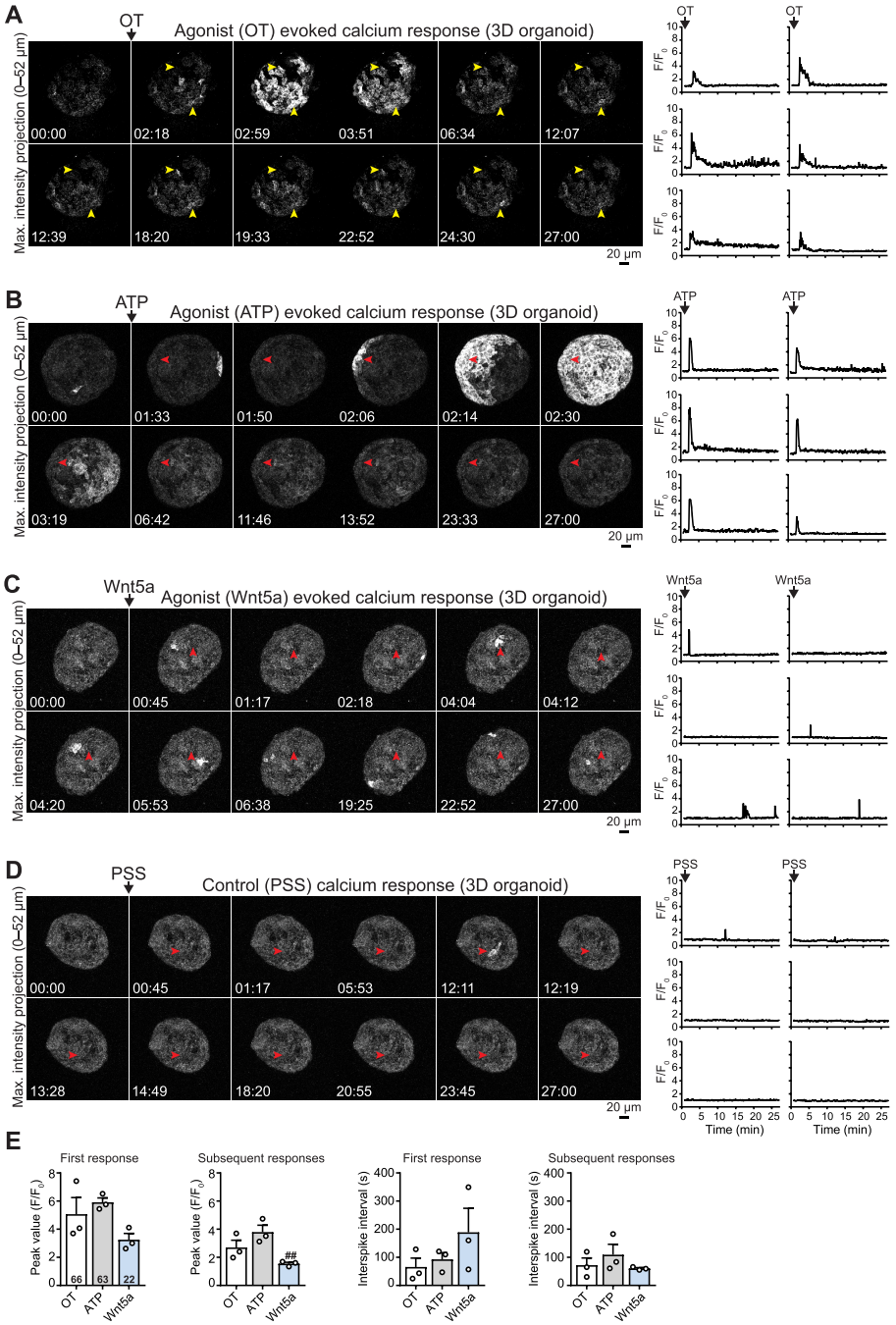

Figure 5. Lineage-specific assessment of agonist evoked Ca^{2+} responses in mammary 3D organoids. Maximum intensity projection showing global cell calcium response (gray) (left), and representative single cell calcium traces showing relative change in fluorescence intensity normalized to baseline (F/F_0) (right) from *GCaMP6f;K5CreERT2* mammary organoids following stimulation with (A) OT, (B) ATP, (C) Wnt5a and (D) PSS. Yellow arrows indicate cells that demonstrate repetitive calcium oscillations (≥2 per imaging series). Red arrows indicate cells that demonstrate a single calcium response. Representative of movies from $n = 3$ (OT, ATP and Wnt5a) and $n = 2$ animals (PSS). (E) Quantitative analysis of calcium responses to agonist stimulation including, peak amplitude (peak value (F/F_0) of initial and secondary calcium spikes), time between consecutive calcium spikes (interspike interval (s)). Numbers denoted in bars indicate the number of cells (out of a total of 75) identified as responding to the corresponding agonist. Graphs show mean ± S.E.M., $n = 3$ independent experiments; ##, $P < 0.05$ in ATP relative to Wnt5a-stimulated primary cells; one-way ANOVA with Bonferroni post-tests.

(Figures 5A,E and S5; Movie S6). Calcium spikes subsequent to the initial calcium store−release event in 3D organoids were generally of lower amplitude and shorter interval relative to 2D primary cells, an effect that may be due to context-dependent influences, as has been shown in 2D versus 3D neuronal cell cultures.[55] Organoid responses to ATP stimulation were characterized by an initial large and transient rise in $[Ca^{2+}]_i$, followed by oscillatory events of lower amplitude, similar to those observed in ATP treated 2D primary cells (Figures 5B,E and S5; Movie S7). As seen for 2D primary cells, a small fraction of GCaMP6f$^+$ cells in 3D organoids displayed low amplitude, irregular calcium responses (as indicated by variable interspike interval) following treatment with Wnt5a (Figures 5C,E and S5; Movie S8), a response that appeared to be distinct from basal

https://dx.doi.org/10.1021/acsptsci.9b00090
ACS Pharmacol. Transl. Sci. 2020, 3, 63−75

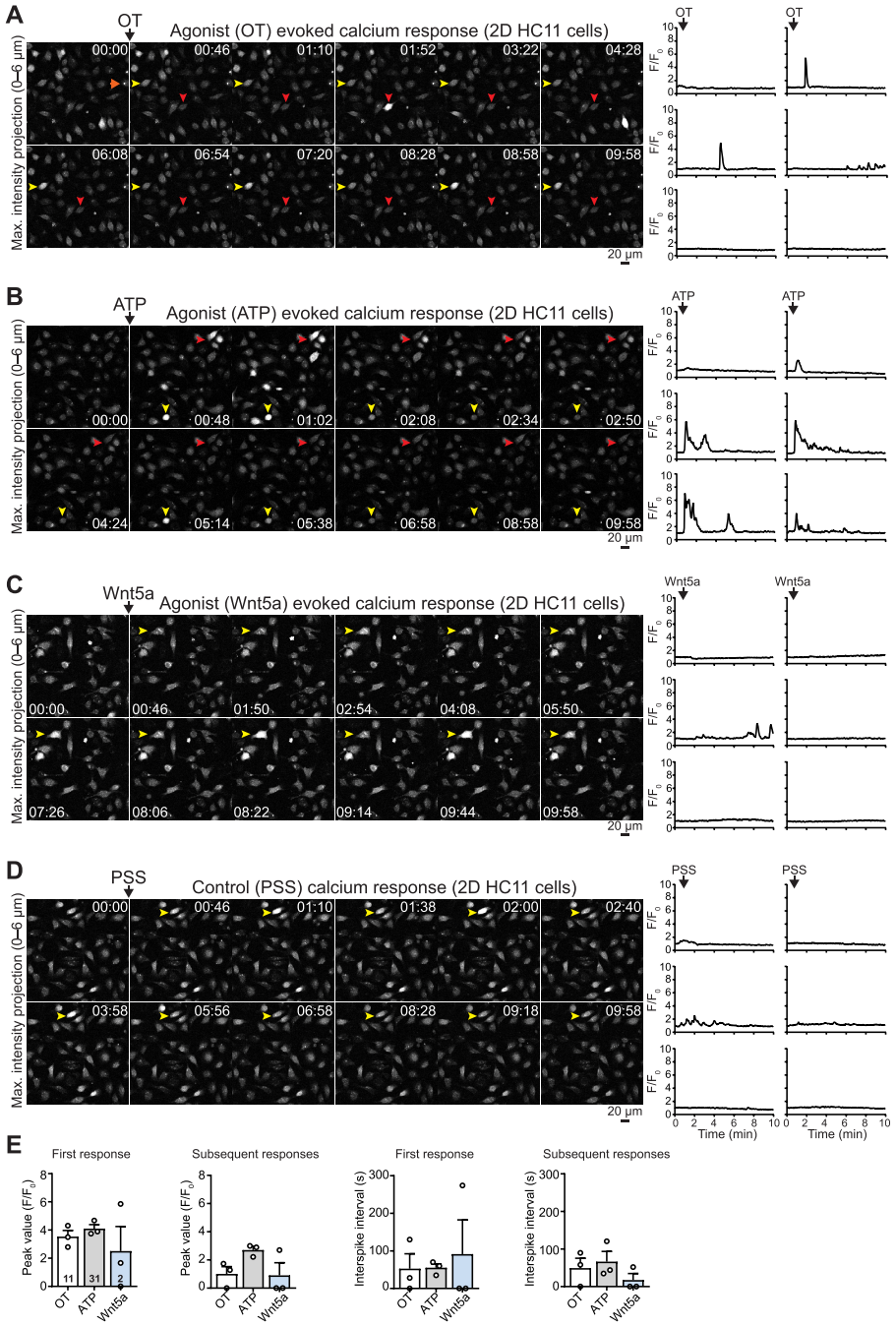

Figure 6. Assessment of calcium signaling in the HC11 immortalized mouse mammary epithelial cell line. Maximum intensity projection showing global cell calcium response (gray) (left), and representative single cell calcium traces showing relative change in fluorescence intensity normalized to baseline (F/F_0) (right) from Fluo4-loaded HC11 cells following stimulation with (A) OT, (B) ATP, (C) Wnt5a, and (D) PSS. Yellow arrows indicate cells that demonstrate repetitive calcium oscillations (≥2 per imaging series). Red arrows indicate cells that demonstrate a single calcium response, representative of movies from $n = 3$ independent experiments. (E) Quantitative analysis of calcium responses to agonist stimulation including, peak amplitude (peak value (F/F_0) of initial and secondary calcium spikes), time between consecutive calcium spikes (interspike interval (s)). Numbers denoted in bars indicate the number of cells (out of a total of 75) identified as responding to the corresponding agonist. Graphs show mean ± S.E.M.; $n = 3$ independent experiments, one-way ANOVA with Bonferroni post-tests.

oscillations observed in PSS (buffer)-treated organoids (Figures 5D and S5; Movie S9). While changes in $[Ca^{2+}]_i$ in GCaMP6f$^+$ basal cells responding to Wnt5a stimulation tended to be delayed in both 2D and 3D primary cells, we did observe one organoid in which a transient and widespread increase in $[Ca^{2+}]_i$ occurred soon after agonist addition (Figure S5 and Movie S10). Recent studies have identified differential, receptor-dependent effects of Wnt5a in distinct mammary stem/progenitor populations.[46] Specifically, Wnt5a inhibits mammary epithelial side branching via ROR2, while promoting epithelial growth in mammosphere formation assays via RYK.[46] It is, therefore, possible that the different calcium responses observed in response to Wnt5a stimulation is associated with the type of receptor expressed by the responding cell(s) and differential contributions to polyclonal organoid cultures (Figure S4B). Using long-term live cell imaging techniques, it would be

https://dx.doi.org/10.1021/acsptsci.9b00090
ACS Pharmacol. Transl. Sci. 2020, 3, 63−75

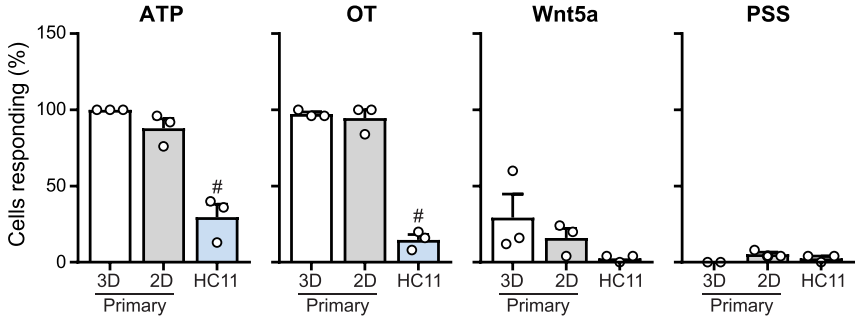

Figure 7. Assessment of ligand-specific responses in 3D and 2D primary and 2D immortalized mammary epithelial cells. Graphs show percent cells responding to ligand stimulation in each model (3D and 2D primary cells and HC11 immortalized cell line). Positive cell calcium responses were determined where maximum signal amplitude (intensity) was >2 AFU. For each ligand, $n = 3$ independent experiments, and PSS, $n = 3$ (2D primary and HC11 cells) or $n = 2$ (3D primary cells) independent experiments (25 randomly selected cells per experiment) were assessed. Graphs show mean ± S.E.M.; #, $P < 0.05$ in 3D and 2D primary cell models versus HC11 immortalized cells, one-way ANOVA with Bonferroni post-tests.

interesting to assess the association between the nature of the Wnt5a-mediated $[Ca^{2+}]_i$ response, Wnt receptor expression, and organoid epithelial side branching.

Collectively, agonist responses in GCaMP6f$^+$ 2D and 3D primary cell models were largely similar and, with respect to OT and ATP, exhibited $[Ca^{2+}]_i$ profiles characteristic of the specific receptors and channels implicated in these signaling pathways.[6,51,56] In order to appreciate the physiological relevance of subtle differences in signaling dynamics, such as lower amplitude, higher frequency oscillations following OT-mediated calcium store−release in organoids, more complex *in situ* calcium imaging studies are required.

Serially passaged, monolayer cultures of immortalized cells are routinely used in early drug discovery and screening studies.[30] Therefore, we also assessed $[Ca^{2+}]_i$ responses in Fluo-4 loaded HC11 cells, a mouse cell line commonly utilized in studies assessing normal mammary epithelial cell biology[57,58] (Figures 6A−E and S4A−C). Only a small number of HC11 cells responded to OT (11/75) (Figures 6A,E and S6; Movie S11) and ATP (31/75) stimulation (Figures 6B,E and S6; Movie S12), and these cells typically lacked the calcium release profile observed in 2D primary cells and organoids (i.e., coordinated initial calcium store release in response to OT stimulation). While Wnt5a-mediated signaling processes have been studied previously in HC11 cells,[59] it was difficult to discern a specific Wnt5a-mediated $[Ca^{2+}]_i$ response (with only 2/75 responding cells identified) (Figures 6C,E and S6; Movie S13) from PSS (buffer) treated cells (Figures 6D and S6; Movie S14). This may be due to the mechanism by which Wnt5a reportedly acts in this cell line, with studies suggesting engagement of the canonical Wnt/β-catenin/TCF signaling pathway as well as transactivation of epidermal growth factor receptor (ErbB1),[59] pathways that may not result in calcium release within the imaging period. To compare all three models, we calculated the percent responding cells to each agonist in 2D primary cells, primary organoids, and the HC11 mammary epithelial cell line (Figure 7). These data reveal that 2D and 3D primary cells are more responsive to all physiological agonists tested. Together, our findings show that, while short-term primary 2D and 3D mammary epithelial cell culture models display similar $[Ca^{2+}]_i$ signaling dynamics in response to physiologically relevant ligand stimulation, the responses in monolayer cultured HC11 cells are less representative of the tissue from which they were originally derived.

CONCLUDING REMARKS

Recognition of the need for more physiologically relevant *in vitro* models in drug discovery research and preclinical development, particularly in the context of anticancer agents, has grown significantly over the past decades.[28−30] At the same time, there is growing appreciation of the value of 4D (x, y, z, and t) organoid and whole tissue imaging in the study of normal cellular and tissue dynamics.[6,60] Here, we have presented an *in vitro* model whereby $[Ca^{2+}]_i$ responses can be assessed following target stimulation in real-time and in both 2D and 3D, while avoiding the limitations associated with the use of synthetic calcium dyes.[15] It is worth noting, while our results suggest 2D primary cells may be a sufficient model for $[Ca^{2+}]_i$ signal analysis in response to direct agonist stimulation, numerous studies have shown distinct advantages of more complex 3D systems, particularly in the assessment of anticancer drug activity.[28] A clear benefit of our 3D organoid model over 2D cultured primary cells, is the potential for its application in studies requiring long-term (up to weeks) monitoring and multiparametric phenotypic analyses. While the *GCaMP6f;K5-CreERT2* mouse model we present in this study allows for detection of relative cytosolic $[Ca^{2+}]_i$ changes in a specific cell type, the rapidly evolving palette of GECIs available means that examination of potential cell−cell interactions through genetic expression of red calcium sensors (e.g., RCaMP) in cocultured cell populations is also possible.[61,62] Coexpression of stably expressed, calcium-independent reference fluorescent proteins with distinct excitation and emission characteristics in the same cell also provides an opportunity for quantitative ratioing, which may be of particular benefit when assessing calcium responses that may be linked to changes in cell shape (e.g., cell-rounding).

Despite the progress made in the development of more complex, physiologically representative 3D models for drug discovery research, a number of barriers to their routine use currently exist, including their adaptation to medium- and high-content screening platforms for improved throughput[63] and the ability to both rapidly acquire and process large sets of imaging data.[28,60,64] With respect to calcium imaging, a number of open-source post-acquisition calcium signal analysis tools have recently become available, including CaSiAn[52] and Flika,[65] with some early analyses performed in 3D systems. The use and improvement of graphical-user-interfaces (GUIs) in many of these publicly available tools increases their accessibility to noncomputational scientists. However, these automated programs, which are often designed for analyzing calcium spikes in

https://dx.doi.org/10.1021/acsptsci.9b00090
ACS Pharmacol. Transl. Sci. 2020, 3, 63−75

excitable cells,[52] can often fail to appropriately detect slow and noisy oscillations in epithelial cell populations, reducing the speed and accuracy of feature extraction. Finally, optimization of 3D matrices that both provide appropriate factors for organoid growth and improve batch to batch consistency, a current limitation of animal derived basement membrane extracts (e.g., Matrigel) and that are compatible with high-throughput automation is also required.[64]

In conclusion, by comparing $[Ca^{2+}]_i$ responses of primary cell derived 3D organoid, 2D primary cells, and an immortalized cell culture model, our findings add to the growing body of literature suggesting that adoption of more complex biological models as tools in drug discovery may help to capture the true heterogeneity of living mammalian systems and improve the translatability of *in vitro* responses in drug discovery and preclinical screening.

MATERIALS AND METHODS

Mice. Animal experimentation was carried out in accordance with the Australian Code for the Care and Use of Animals for Scientific Purposes and the Queensland Animal Care and Protection Act (2001), with local ethics committee approval. Animals were housed in a specific-pathogen-free (SPF) facility in individually ventilated cages with standard enrichment under a 12:12 h light−dark cycle. Regular mouse chow and water were available ad libitum. K5-CreERT2 mice (B6N.129S6(Cg)-Krt5$^{tm1.1(cre/ERT2)Blh}$/J, stock no. 029155) were sourced from The Jackson Laboratory (Bar Harbor, ME). GCaMP6f-fl mice (B6J.Cg-Gt(ROSA)26Sor$^{tm95.1(CAG-GCaMP6f)Hze}$/MwarJ) were a gift from Dr. James W. Putney Jr. (National Institutes of Environmental Health Sciences, NC). C57BL6 (used for tissue-clearing studies) were obtained from the Animal Resources Centre (Western Australia). Mice were maintained on a C57BL6 background as heterozygotes. Female animals were used experimentally and were sacrificed postpuberty, between 21 and 33 weeks of age.

DNA extracted from mouse toe, ear, or tail was used for genotyping with the following primers: K5-CreERT2 5′-GGA GGA AGT CAG AAC CAG GAC-3′, 5′-GCA AGA CCC TGG TCC TCA C-3′, 5′-ACC GGC CTT ATT CCA AGC-3′ (PCR product size: wild type 322 bp, mutant 190 bp), and GCaMP6f-fl 5′-CTC TGC TGC CTC CTG GCT TCT-3′, 5′-CGA GGC GGA TCA CAA GCA ATA-3′, and 5′-TCA ATG GGC GGG GGT CGT T-3′ (PCR product size: wild type 330 bp, mutant 250 bp).

GCaMP6f was induced by administering 1.5 mg of tamoxifen (Sigma, T6548) prepared in sunflower seed oil (Sigma, S5007) and ethanol (10%) via intraperitoneal injection at 28, 56, and 58 days of age.

Mammary Organoids. Mammary organoids were created from the fourth mammary glands (with inguinal lymph nodes removed) of *GCaMP6f;K5CreERT2* virgin mice, as previously described,[6,32] with the following modifications. Tissue was dissociated by chopping briefly with scalpel blades and placing in a digestion mix before transferring to a gentleMACS Dissociator (Miltenyi Biotec) and running program 37C_m_LDK_1 (gentle mechanical agitation at 37 °C for 31 min). Organoid medium was replaced 3 times per week, and organoids were maintained for 7−21 days. Organoids were nonenzymatically passaged in fresh Cultrex Reduced Growth Factor Basement Membrane Extract (R&D Systems, RD343300501, Lot: 39795F17) into a μ-Dish (Ibidi, 81158) 1−2 days prior to live imaging.

Organoids were incubated with CellTracker Red (6 μM, ThermoFisher Scientific, C34552) at 37 °C with 5% CO_2 for 20−30 min prior to imaging. Live imaging was performed in physiological salt solution (PSS, pH 7.3−7.4) [HEPES (10 mM), KCl (5.9 mM), $MgCl_2$ (1.4 mM), NaH_2PO_4 (1.2 mM), $NaHCO_3$ (5 mM), NaCl (140 mM), glucose (11.5 mM), and $CaCl_2$ (1.8 mM)], and organoids were stimulated with adenosine 5′-triphosphate (ATP, 100 μM, Sigma, A6419), oxytocin (85 nM, Sigma, O3251), Wnt5a (100 ng/mL, R&D Systems, 645-WN-010), or PSS. Images were acquired every 4.060−4.084 s (total scan time = 27 min) on an Olympus FV3000 inverted confocal laser scanning microscope with resonant scanner and using a UPLSAPO 30×/1.05 silicone objective. Agonist additions were made between 40−50 s from the start of imaging.

Primary Cells. 2D primary cell cultures were prepared in parallel to organoids. Following mammary gland dissociation, cells were counted and suspended in 2D primary cell culture media [DMEM/F12 (ThermoFisher Scientific, 11330032) with 10% FCS and 1× penicillin/streptomycin (ThermoFisher Scientific, 15140122)]. Approximately 2.5 × 10^4 cells/5 μL were spotted on the bottom of an imaging dish and left for 4−6 h at 37 °C with 5% CO_2 in a humidified incubator to adhere before the addition of 2D primary cell culture media.[51] 2D primary cell experiments were performed within 24 h of plating.

For live imaging experiments, primary cells were incubated with CellTracker Red and stimulated with agonists as described in the above section. Images were acquired every 2 s (total scan time 10 min) as described for mammary organoids. Agonist additions were made approximately 40 s from the commencement of imaging.

HC11 Cell Culture. Immortalized HC11 mammary epithelial cells,[58] a gift from Prof. Melissa Brown (The University of Queensland, Australia), were cultured in RPMI-1640 (Sigma, R8758) supplemented with fetal calf serum (Thermo Fisher Scientific, 10099141, 10%), bovine insulin (Sigma, I6634, 5 μg/mL), and murine epidermal growth factor (Sigma, E4127, 10 ng/mL). Cells were maintained at 37 °C with 5% CO_2 in a humidified environment and routinely tested negative to mycoplasma infection (MycoAlert; Lonza, LT07−218).

For calcium studies, HC11 cells were loaded with 4 μM Fluo4-AM (F14201, ThermoFisher Scientific) for 20 min at 37 °C. Following dye incubation, cells were washed 1× with PSS containing 0.3% BSA, followed by PSS only. Agonist stimulation and image acquisition were performed as detailed above for 2D primary cell experiments.

Immunofluorescence Staining. HC11 and *GCaMP6f;K5-CreERT2* 2D primary cells were washed gently with phosphate-buffered saline (PBS), fixed in paraformaldehyde (PFA, 4%) for 15 min at room temperature, and permeabilized in ice cold methanol for 10 min on ice. Cells were blocked for 1 h at room temperature before primary antibody incubation overnight at 4 °C. The following primary antibodies were used in this study: chicken anti-green fluorescent protein (GFP; 1:2000, Abcam, ab13970), rabbit anti-keratin 5 (K5; 1:100, Biolegend, 905503), rat anti-keratin 8 (K8; 1:200, Developmental Studies Hybridoma Bank, TROMA-I), and rabbit anti-p63 (1:100, Abcam, ab124762). The following secondary antibodies were used in this study (at a dilution of 1:500): goat anti-chicken Alexa Fluor 488 (Life Technologies, A11039), goat anti-rat Cyanine3 (Life Technologies, A10522), goat anti-rabbit Alexa Fluor 647 (Life Technologies, A21245), and goat anti-mouse Alexa Fluor 647

https://dx.doi.org/10.1021/acsptsci.9b00090
ACS Pharmacol. Transl. Sci. 2020, 3, 63−75

(Life Technologies, A21236). Nuclei were counterstained with DAPI (5 μg/mL) for 15 min at room temperature. Image acquisition was performed using an Olympus FV3000 laser scanning confocal microscope with UPLSAPO 20×/0.75 and UPLSAPO 10×/0.4 air objective lenses. Post-acquisition image visualization and processing was performed with ImageJ (v1.52e, National Institutes of Health).[66] Images have been brightness and contrast adjusted for publication.

GCaMP6f;K5CreERT2 organoids were fixed in PFA 4% for 30 min at room temperature and permeabilized in PBS with 0.2% Triton X-100 for 15 min at 37 °C. Organoids were blocked for 1 h at 37 °C before primary antibody incubation for 2 h at 37 °C. The following primary antibodies were used in this study: chicken anti-green fluorescent protein (GFP; 1:2000), rabbit anti-keratin 5 (K5; 1:150, Biolegend, 905503), rat anti-keratin 8 (K8; 1:50−1:100), and rabbit anti-p63 (1:100). Nuclei were counterstained with DAPI (5 μg/mL) for 15 min at room temperature. Image acquisition and processing was performed as described above for 2D cells.

Tissue Clearing. Mouse mammary tissue was dissected and fixed for 6−9 h in neutral buffered formalin solution (10%, Sigma, HT501128) and tissue clearing performed using a modified CUBIC protocol (CUBIC 1A) as previously described.[22,67,68] The following primary antibodies were used in this study: chicken anti-green fluorescent protein (GFP; 1:2000), rat anti-Keratin 8 (K8; 1:50) and rabbit anti-alpha smooth muscle actin (SMA; 1:300, Abcam, ab5694). Nuclei were counterstained with DAPI (5 μg/mL) for 2 h at room temperature. Following staining, cleared tissue was immersed in CUBIC Reagent 2 for a minimum of 24 h prior to imaging. Image acquisition was performed using an Olympus FV3000 laser scanning confocal microscope with UPLSAPO 20×/0.75 and UPLSAPO 10×/0.4 air objective lenses. Post-acquisition image visualization and processing was performed with ImageJ (v1.52e, National Institutes of Health),[66] and denoising was performed as previously described.[69]

RNA Analysis. RNA extractions were performed using the RNeasy Plus Mini Kit with gDNA eliminator columns according to the manufacturer's instructions (Qiagen, 74134). Briefly, HC11 cells were lysed directly in RLT Buffer Plus, while fresh frozen mammary gland tissue was first crushed to a fine powder using a mortar and pestle over dry ice before suspending in RLT Buffer Plus. HC11 cDNA was prepared using the Omniscript RT Kit (Qiagen, 205113), while cDNA from fresh frozen tissue was prepared using the Quantitect RT Kit, which includes an additional gDNA removal step (Qiagen, 205311). Gene expression levels were assessed using the following prevalidated TaqMan Gene Expression Assays (Applied Biosystems): *Oxtr* (Mm01182684), *P2ry1* (Mm02619947), *P2ry2* (Mm02619978), *P2ry6* (Mm02620937), *P2rx1* (Mm00435460), *P2rx4* (Mm00501787), *P2rx5* (Mm00473677), *Ryk* (Mm01238551), *Ror1* (Mm00443462), and *Ror2* (Mm00443470). Ct values were then normalized to the reference gene, 18S rRNA, and relative mRNA levels are expressed as −ΔCt.[53]

Cell Ca^{2+} Analysis. Calcium signals were extracted in ImageJ using the Time Series Analyzer V3 plugin. Maximum intensity projections were created from image stacks and 25 predefined regions of interest were assigned at random based on the first imaging frame (prior to agonist stimulation). Changes in calcium signal intensity were calculated based on starting fluorescence (F/F_0), and calcium traces were plotted in GraphPad Prism (v7.03). Images have been brightness- and contrast-adjusted for publication. For analysis of calcium spike trains, normalized fluorescence values (F/F_0) were imported into CaSiAn.[52] Nonresponding cells were considered to have a peak amplitude (intensity) less than 2 AFU and were excluded from further analyses. Automatic peak and nadir detection was performed in CaSiAn using a peak threshold of 15% of the maximum peak amplitude. In some cases, however, the program failed to accurately detect calcium spikes (Figure S7A). Calcium oscillations in basal epithelial cells are slow, and unlike many other characterized cell types, successive calcium spikes can arrive before the signal has returned to baseline levels (Figure S7B (i−iii)), leading to problems in peak and nadir detection.

STUDY LIMITATION

This is a proof-of-concept study comparing agonist responses in biologically complex versus traditional cell-based assays. The authors acknowledge a limitation of this study is the assessment of a single concentration of each agonist for the activity readout in each model. Subsequent studies assessing concentration−response relationships are warranted.

ASSOCIATED CONTENT

Supporting Information

The Supporting Information is available free of charge at https://pubs.acs.org/doi/10.1021/acsptsci.9b00090.

Immunofluorescence staining of organoid, 2D primary cells, 2D mammary primary epithelial cell agonist calcium traces, relative (−ΔCt) mRNA levels of selected lysates, 3D mammary organoid agonist calcium traces, 2D HC11 mammary epithelial cell line agonist calcium traces, percentage of cells excluded from analysis due to failed/inappropriate spike detection, representative spike detection traces (PDF)

Movie S1: 3D visualization of mammary gland tissues; Movies S2−S5: response of live 2D mammary epithelial cells to oxytocin, ATP, Wnt5a, and PSS; Movies S6−S9: response of mammary organoid to oxytocin, ATP, Wnt5a, and PSS; Movie S10: atypical response in a live mammary organoid to Wnt5a; Movies S11−S14: response in live HC11 immortalized mammary epithelial cells loaded with Fluo-4 to oxytocin, ATP, Wnt5a, and PSS (ZIP)

AUTHOR INFORMATION

Corresponding Authors

Teneale A. Stewart − *Faculty of Medicine, Mater Research-The University of Queensland, Brisbane 4102, Australia; Translational Research Institute, Brisbane 4102, Australia*; Email: teneale.stewart@mater.uq.edu.au

Felicity M. Davis − *Faculty of Medicine, Mater Research-The University of Queensland, Brisbane 4102, Australia; Translational Research Institute, Brisbane 4102, Australia*; orcid.org/0000-0001-9112-118X; Email: f.davis@uq.edu.au

Complete contact information is available at: https://pubs.acs.org/10.1021/acsptsci.9b00090

Author Contributions

Conceptualization, F.M.D. and T.A.S.; methodology, F.M.D. and T.A.S.; experimental investigation, T.A.S. and F.M.D.; writing, T.A.S. and F.M.D.; project administration, F.M.D.; funding acquisition, F.M.D. All authors have given approval to the final version of the manuscript.

https://dx.doi.org/10.1021/acsptsci.9b00090
ACS Pharmacol. Transl. Sci. 2020, 3, 63−75

Funding

This work was supported by the National Health and Medical Research Council [1141008 and 1138214 (F.M.D.)] and the National Stem Cell Foundation of Australia (Metcalf Award to F.M.D). Funding was also provided by the Mater Foundation (Equity Trustees/AE Hingeley Trust).

Notes

The authors declare no competing financial interest.

■ ACKNOWLEDGMENTS

We gratefully acknowledge the Translational Research Institute Imaging and Biological Resource core facilities that enabled much of this work. We thank Mr. Alex Stevenson (Mater Research-UQ) for his assistance in colony management, genotyping, and laboratory management, Dr. Bethan Lloyd-Lewis (Institut Curie) for her expertise in organoid culture, and Dr. Jerome Boulanger (MRC Laboratory of Molecular Biology) for the 3D denoising algorithm.

■ ABBREVIATIONS

2D, two-dimensional; 3D, three-dimensional; ATP, adenosine 5′-triphosphate; GECI, genetically encoded calcium indicator; GFP, green fluorescent protein; GPCR, G-protein coupled receptor; K5, keratin 5; K8, keratin 8; OT, oxytocin; ROR2, receptor tyrosine kinase-like orphan receptor 2; SMA, smooth muscle actin; Wnt5a, wingless-type MMTV integration site 5a

■ REFERENCES

(1) van Staveren, W. C. G., Solís, D. Y. W., Hébrant, A., Detours, V., Dumont, J. E., and Maenhaut, C. (2009) Human cancer cell lines: Experimental models for cancer cells in situ? For cancer stem cells? *Biochim. Biophys. Acta, Rev. Cancer 1795*, 92−103.

(2) Riedl, A., Schlederer, M., Pudelko, K., Stadler, M., Walter, S., Unterleuthner, D., Unger, C., Kramer, N., Hengstschläger, M., Kenner, L., Pfeiffer, D., Krupitza, G., and Dolznig, H. (2017) Comparison of cancer cells in 2D vs 3D culture reveals differences in AKT-mTOR-S6K signaling and drug responses. *J. Cell Sci. 130*, 203−218.

(3) Weigelt, B., Lo, A. T., Park, C. C., Gray, J. W., and Bissell, M. J. (2010) HER2 signaling pathway activation and response of breast cancer cells to HER2-targeting agents is dependent strongly on the 3D microenvironment. *Breast Cancer Res. Treat. 122*, 35−43.

(4) Furuta, S., and Bissell, M. J. (2016) Pathways involved in formation of mammary organoid architecture have keys to understanding drug resistance and to discovery of druggable targets. *Cold Spring Harbor Symp. Quant. Biol. 81*, 207−217.

(5) Fosque, B. F., Sun, Y., Dana, H., Yang, C. T., Ohyama, T., Tadross, M. R., Patel, R., Zlatic, M., Kim, D. S., Ahrens, M. B., Jayaraman, V., Looger, L. L., and Schreiter, E. R. (2015) Labeling of active neural circuits in vivo with designed calcium integrators. *Science 347*, 755−760.

(6) Stevenson, A. J., Vanwalleghem, G., Stewart, T. A., Condon, N. D., Lloyd-Lewis, B., Marino, N., Putney, J. W., Scott, E. K., Ewing, A. D., and Davis, F. M. (2019) Multiscale activity imaging in the mammary gland reveals how oxytocin enables lactation. bioRxiv 657510; *bioRxiv e-Print archive*. https://doi.org/10.1101/657510 (accessed Nov 24, 2019).

(7) Tuveson, D., and Clevers, H. (2019) Cancer modeling meets human organoid technology. *Science 364*, 952−955.

(8) Lancaster, M. A., and Huch, M. (2019) Disease modelling in human organoids. *Dis. Models Mech. 12*, dmm039347.

(9) Sachs, N., de Ligt, J., Kopper, O., Gogola, E., Bounova, G., Weeber, F., Balgobind, A. V., Wind, K., Gracanin, A., Begthel, H., Korving, J., van Boxtel, R., Duarte, A. A., Lelieveld, D., van Hoeck, A., Ernst, R. F., Blokzijl, F., Nijman, I. J., Hoogstraat, M., van de Ven, M., Egan, D. A., Zinzalla, V., Moll, J., Boj, S. F., Voest, E. E., Wessels, L., van Diest, P. J., Rottenberg, S., Vries, R. G. J., Cuppen, E., and Clevers, H. (2018) A Living Biobank of Breast Cancer Organoids Captures Disease Heterogeneity. *Cell 172*, 373−386.

(10) Broutier, L., Mastrogiovanni, G., Verstegen, M. M. A., Francies, H. E., Gavarró, L. M., Bradshaw, C. R., Allen, G. E., Arnes-Benito, R., Sidorova, O., Gaspersz, M. P., Georgakopoulos, N., Koo, B. K., Dietmann, S., Davies, S. E., Praseedom, R. K., Lieshout, R., IJzermans, J. N. M., Wigmore, S. J., Saeb-Parsy, K., Garnett, M. J., Van Der Laan, L. J. W., and Huch, M. (2017) Human primary liver cancer-derived organoid cultures for disease modeling and drug screening. *Nat. Med. 23*, 1424−1435.

(11) Kim, M., Mun, H., Sung, C. O., Cho, E. J., Jeon, H. J., Chun, S. M., Jung, D. J., Shin, T. H., Jeong, G. S., Kim, D. K., Choi, E. K., Jeong, S. Y., Taylor, A. M., Jain, S., Meyerson, M., and Jang, S. J. (2019) Patient-derived lung cancer organoids as in vitro cancer models for therapeutic screening. *Nat. Commun. 10*, 3991.

(12) Chan, W. Y., McKinzie, D. L., Bose, S., Mitchell, S. N., Witkin, J. M., Thompson, R. C., Christopoulos, A., Lazareno, S., Birdsall, N. J. M., Bymaster, F. P., and Felder, C. C. (2008) Allosteric modulation of the muscarinic M4 receptor as an approach to treating schizophrenia. *Proc. Natl. Acad. Sci. U. S. A. 105*, 10978−10983.

(13) Qin, C. X., May, L. T., Li, R., Cao, N., Rosli, S., Deo, M., Alexander, A. E., Horlock, D., Bourke, J. E., Yang, Y. H., Stewart, A. G., Kaye, D. M., Du, X. J., Sexton, P. M., Christopoulos, A., Gao, X. M., and Ritchie, R. H. (2017) Small-molecule-biased formyl peptide receptor agonist compound 17b protects against myocardial ischaemia-reperfusion injury in mice. *Nat. Commun. 8*, 14232.

(14) Monteith, G. R., and Bird, G. S. J. (2005) Techniques: High-throughput measurement of intracellular Ca2+ - Back to basics. *Trends Pharmacol. Sci. 26*, 218−223.

(15) Wu, N., Nishioka, W. K., Derecki, N. C., and Maher, M. P. (2019) High-throughput-compatible assays using a genetically-encoded calcium indicator. *Sci. Rep. 9*, 12692.

(16) Bassett, J. J., and Monteith, G. R. (2017) Genetically Encoded Calcium Indicators as Probes to Assess the Role of Calcium Channels in Disease and for High-Throughput Drug Discovery. *Adv. Pharmacol. 79*, 141−171.

(17) Suzuki, J., Kanemaru, K., and Iino, M. (2016) Genetically Encoded Fluorescent Indicators for Organellar Calcium Imaging. *Biophys. J. 111*, 1119−1131.

(18) Lloyd-Lewis, B., Harris, O. B., Watson, C. J., and Davis, F. M. (2017) Mammary stem cells: Premise, properties and perspectives. *Trends Cell Biol. 27*, 556−567.

(19) Inman, J. L., Robertson, C., Mott, J. D., and Bissell, M. J. (2015) Mammary gland development: cell fate specification, stem cells and the microenvironment. *Development 142*, 1028−1042.

(20) Lilja, A. M. M., Rodilla, V., Huyghe, M., Hannezo, E., Landragin, C., Renaud, O., Leroy, A., Rulands, S., Simons, B. D. D., and Fre, S. (2018) Clonal analysis of Notch1-expressing cells reveals the existence of unipotent stem cells that retain long-term plasticity in the embryonic mammary gland. *Nat. Cell Biol. 20*, 677−687.

(21) Wuidart, A., Sifrim, A., Fioramonti, M., Matsumura, S., Brisebarre, A., Brown, D., Centonze, A., Dannau, A., Dubois, C., Van Keymeulen, A., Voet, T., and Blanpain, C. C. (2018) Early lineage segregation of multipotent embryonic mammary gland progenitors. *Nat. Cell Biol. 20*, 666−676.

(22) Stewart, T. A., Hughes, K., Stevenson, A. S. J., Marino, N., Ju, A. J. L., Morehead, M., and Davis, F. M. (2019) Mammary mechanobiology: mechanically-activated ion channels in lactation and involution. bioRxiv 649038; *bioRxiv e-Print archive*. https://doi.org/10.1101/649038 (accessed Nov 24, 2019).

(23) Peuhu, E., Virtakoivu, R., Mai, A., Wärri, A., and Ivaska, J. (2017) Epithelial vimentin plays a functional role in mammary gland development. *Development 144*, 4103−4113.

(24) Williams, C., Helguero, L., Edvardsson, K., Haldosén, L. A., and Gustafsson, J. Å. (2009) Gene expression in murine mammary epithelial stem cell-like cells shows similarities to human breast cancer gene expression. *Breast Cancer Res. 11*, R26.

(25) Weaver, V. M., Petersen, O. W., Wang, F., Larabell, C. A., Briand, P., Damsky, C., and Bissell, M. J. (1997) Reversion of the malignant

phenotype of human breast cells in three- dimensional culture and in vivo by integrin blocking antibodies. *J. Cell Biol. 137*, 231−245.
(26) Petersen, O. W., Ronnov-Jessen, L., Howlett, A. R., and Bissell, M. J. (1992) Interaction with basement membrane serves to rapidly distinguish growth and differentiation pattern of normal and malignant human breast epithelial cells. *Proc. Natl. Acad. Sci. U. S. A. 89*, 9064−9068.
(27) Pickl, M., and Ries, C. H. (2009) Comparison of 3D and 2D tumor models reveals enhanced HER2 activation in 3D associated with an increased response to trastuzumab. *Oncogene 28*, 461−468.
(28) Langhans, S. A. (2018) Three-dimensional in vitro cell culture models in drug discovery and drug repositioning. *Front. Pharmacol. 9*, 6.
(29) Horvath, P., Aulner, N., Bickle, M., Davies, A. M., Nery, E., Ebner, D., Montoya, M. C., Östling, P., Pietiäinen, V., Price, L. S., Shorte, S. L., Turcatti, G., von Schantz, C., and Carragher, N. O. (2016) Screening out irrelevant cell-based models of disease. *Nat. Rev. Drug Discovery 15*, 751−769.
(30) Breslin, S., and O'Driscoll, L. (2013) Three-dimensional cell culture: The missing link in drug discovery. *Drug Discovery Today 18*, 240−249.
(31) Shamir, E. R., and Ewald, A. J. (2014) Three-dimensional organotypic culture: Experimental models of mammalian biology and disease. *Nat. Rev. Mol. Cell Biol. 15*, 647−664.
(32) Jardé, T., Lloyd-Lewis, B., Thomas, M., Kendrick, H., Melchor, L., Bougaret, L., Watson, P. D. D., Ewan, K., Smalley, M. J. J., and Dale, T. C. C. (2016) Wnt and Neuregulin1/ErbB signalling extends 3D culture of hormone responsive mammary organoids. *Nat. Commun. 7*, 13207.
(33) Jamieson, P. R., Dekkers, J. F., Rios, A. C., Fu, N. Y., Lindeman, G. J., and Visvader, J. E. (2017) Derivation of a robust mouse mammary organoid system for studying tissue dynamics. *Development 144*, 1065−1071.
(34) Davis, F. M., Azimi, I., Faville, R. A., Peters, A. A., Jalink, K., Putney, J. W., Goodhill, G. J., Thompson, E. W., Roberts-Thomson, S. J., and Monteith, G. R. (2014) Induction of epithelial-mesenchymal transition (EMT) in breast cancer cells is calcium signal dependent. *Oncogene 33*, 2307−2316.
(35) Bootman, M. D., and Roderick, H. L. (2011) Using calcium imaging as a readout of GPCR activation. *Methods Mol. Biol. 746*, 277−96.
(36) Chen, T.-W., Wardill, T. J., Sun, Y., Pulver, S. R., Renninger, S. L., Baohan, A., Schreiter, E. R., Kerr, R. A., Orger, M. B., Jayaraman, V., Looger, L. L., Svoboda, K., and Kim, D. S. (2013) Ultrasensitive fluorescent proteins for imaging neuronal activity. *Nature 499*, 295−300.
(37) Stokes, D. G., Liu, G., Dharmavaram, R., Hawkins, D., Piera-Velazquez, S., and Jimenez, S. A. (2001) Regulation of type-II collagen gene expression during human chondrocyte de-differentiation and recovery of chondrocyte-specific phenotype in culture involves Sry-type high-mobility-group box (SOX) transcription factors. *Biochem. J. 360*, 461−470.
(38) Bissell, M. J., Rizki, A., and Mian, I. S. (2003) Tissue architecture: The ultimate regulator of breast epithelial function. *Curr. Opin. Cell Biol. 15*, 753−762.
(39) Wang, F., Weaver, V. M., Petersen, O. W., Larabell, C. A., Dedhar, S., Briand, P., Lupu, R., and Bissell, M. J. (1998) Reciprocal interactions between β1-integrin and epidermal growth factor receptor in three-dimensional basement membrane breast cultures: A different perspective in epithelial biology. *Proc. Natl. Acad. Sci. U. S. A. 95*, 14821−14826.
(40) Gimpl, G., and Fahrenholz, F. (2001) The oxytocin receptor system: structure, function, and regulation. *Physiol. Rev. 81*, 629−683.
(41) Burnstock, G., Knight, G. E., and Greig, A. V. H. (2012) Purinergic signaling in healthy and diseased skin. *J. Invest. Dermatol. 132*, 526−546.
(42) Di Virgilio, F., Sarti, A. C., Falzoni, S., De Marchi, E., and Adinolfi, E. (2018) Extracellular ATP and P2 purinergic signalling in the tumour microenvironment. *Nat. Rev. Cancer 18*, 601−618.
(43) Nakano, H., Furuya, K., Furuya, S., and Yamagishi, S. (1997) Involvement of P2-purinergic receptors in intracellular Ca2+ responses and the contraction of mammary myoepithelial cells. *Pfluegers Arch. 435*, 1−8.
(44) Ohtomo, K., Shatos, M. A., Vrouvlianis, J., Li, D., Hodges, R. R., and Dartt, D. A. (2011) Increase of intracellular Ca 2+ by purinergic receptors in cultured rat lacrimal gland myoepithelial cells. *Invest. Ophthalmol. Visual Sci. 52*, 9503−9515.
(45) Roarty, K., and Serra, R. (2007) Wnt5a is required for proper mammary gland development and TGF-beta-mediated inhibition of ductal growth. *Development 134*, 3929−3939.
(46) Kessenbrock, K., Smith, P., Steenbeek, S. C., Pervolarakis, N., Kumar, R., Minami, Y., Goga, A., Hinck, L., and Werb, Z. (2017) Diverse regulation of mammary epithelial growth and branching morphogenesis through noncanonical Wnt signaling. *Proc. Natl. Acad. Sci. U. S. A. 114*, 3121−3126.
(47) McQuate, A., Latorre-Esteves, E., and Barria, A. (2017) A Wnt/Calcium Signaling Cascade Regulates Neuronal Excitability and Trafficking of NMDARs. *Cell Rep. 21*, 60−69.
(48) Thrasivoulou, C., Millar, M., and Ahmed, A. (2013) Activation of intracellular calcium by multiple Wnt ligands and translocation of β-catenin into the nucleus: A convergent model of Wnt/Ca2+and Wnt/β-catenin pathways. *J. Biol. Chem. 288*, 35651−35659.
(49) Wang, Q., Symes, A. J., Kane, C. A., Freeman, A., Nariculam, J., Munson, P., Thrasivoulou, C., Masters, J. R. W., and Ahmed, A. (2010) A novel role for Wnt/Ca2+ signaling in actin cytoskeleton remodeling and cell motility in prostate cancer. *PLoS One 5*, e10456.
(50) Ji, H., Goode, R. J. A., Vaillant, F., Mathivanan, S., Kapp, E. A., Mathias, R. A., Lindeman, G. J., Visvader, J. E., and Simpson, R. J. (2011) Proteomic profiling of secretome and adherent plasma membranes from distinct mammary epithelial cell subpopulations. *Proteomics 11*, 4029−4039.
(51) Davis, F. M., Janoshazi, A., Janardhan, K. S., Steinckwich, N., D'Agostin, D. M., Petranka, J. G., Desai, P. N., Roberts-Thomson, S. J., Bird, G. S., Tucker, D. K., Fenton, S. E., Feske, S., Monteith, G. R., and Putney, J. W. (2015) Essential role of Orai1 store-operated calcium channels in lactation. *Proc. Natl. Acad. Sci. U. S. A. 112*, 5827−5832.
(52) Moein, M., Grzyb, K., Gonçalves Martins, T., Komoto, S., Peri, F., Crawford, A. D., d'Herouel, A. F., and Skupin, A. (2018) CaSiAn: A calcium signaling analyzer tool. *Bioinformatics 34*, 3052−3054.
(53) Davis, F. M., Kenny, P. A., Soo, E. T. L., van Denderen, B. J. W., Thompson, E. W., Cabot, P. J., Parat, M. O., Roberts-Thomson, S. J., and Monteith, G. R. (2011) Remodeling of purinergic receptor-mediated Ca 2+ signaling as a consequence of EGF-induced epithelial-mesenchymal transition in breast cancer cells. *PLoS One 6*, e23464.
(54) Bach, K., Pensa, S., Grzelak, M., Hadfield, J., Adams, D. J. J., Marioni, J. C. C., and Khaled, W. T. T. (2017) Differentiation dynamics of mammary epithelial cells revealed by single-cell RNA sequencing. *Nat. Commun. 8*, 2128.
(55) Lai, Y., Cheng, K., and Kisaalita, W. (2012) Three Dimensional Neuronal Cell Cultures More Accurately Model Voltage Gated Calcium Channel Functionality in Freshly Dissected Nerve Tissue. *PLoS One 7*, e45074.
(56) Davis, F. M., Peters, A. A., Grice, D. M., Cabot, P. J., Parat, M. O., Roberts-Thomson, S. J., and Monteith, G. R. (2012) Non-stimulated, agonist-stimulated and store-operated ca2+ influx in MDA-MB-468 breast cancer cells and the effect of EGF-induced EMT on calcium entry. *PLoS One 7*, e36923.
(57) Ball, R. K., Friis, R. R., Schoenenberger, C. A., Doppler, W., and Groner, B. (1988) Prolactin regulation of beta-casein gene expression and of a cytosolic 120-kd protein in a cloned mouse mammary epithelial cell line. *EMBO J. 7*, 2089−2095.
(58) Hynes, N. E. E., Taverna, D., Harwerth, I. M. M., Ciardiello, F., Salomon, D. S. S., Yamamoto, T., and Groner, B. (1990) Epidermal growth factor receptor, but not c-erbB-2, activation prevents lactogenic hormone induction of the beta-casein gene in mouse mammary epithelial cells. *Mol. Cell. Biol. 10*, 4027−34.

https://dx.doi.org/10.1021/acsptsci.9b00090
ACS Pharmacol. Transl. Sci. 2020, 3, 63−75

(59) Civenni, G., Holbro, T., and Hynes, N. E. (2003) Wntl and Wnt5a induce cyclin D1 expression through ErbB1 transactivation in HC11 mammary epithelial cells. *EMBO Rep. 4*, 166−171.
(60) Rios, A. C., and Clevers, H. (2018) Imaging organoids: A bright future ahead. *Nat. Methods 15*, 24−26.
(61) Akerboom, J., Calderón, N. C., Tian, L., Wabnig, S., Prigge, M., Tolö, J., Gordus, A., Orger, M. B., Severi, K. E., Macklin, J. J., Patel, R., Pulver, S. R., Wardill, T. J., Fischer, E., Schüler, C., Chen, T. W., Sarkisyan, K. S., Marvin, J. S., Bargmann, C. I., Kim, D. S., Kügler, S., Lagnado, L., Hegemann, P., Gottschalk, A., Schreiter, E. R., and Looger, L. L. (2013) Genetically encoded calcium indicators for multi-color neural activity imaging and combination with optogenetics. *Front. Mol. Neurosci. 6*, 2.
(62) Zhao, Y., Araki, S., Wu, J., Teramoto, T., Chang, Y. F., Nakano, M., Abdelfattah, A. S., Fujiwara, M., Ishihara, T., Nagai, T., and Campbell, R. E. (2011) An expanded palette of genetically encoded Ca2+ indicators. *Science (Washington, DC, U. S.) 333*, 1888−1891.
(63) Mattiazzi Usaj, M., Styles, E. B., Verster, A. J., Friesen, H., Boone, C., and Andrews, B. J. (2016) High-Content Screening for Quantitative Cell Biology. *Trends Cell Biol. 26*, 598−611.
(64) Booij, T. H., Price, L. S., and Danen, E. H. J. (2019) 3D Cell-Based Assays for Drug Screens: Challenges in Imaging, Image Analysis, and High-Content Analysis. *SLAS Discovery 24*, 615−627.
(65) Ellefsen, K. L., Lock, J. T., Settle, B., Karsten, C. A., and Parker, I. (2019) Applications of FLIKA, a Python-based image processing and analysis platform, for studying local events of cellular calcium signaling. *Biochim. Biophys. Acta, Mol. Cell Res. 1866*, 1171−1179.
(66) Schindelin, J., Arganda-Carreras, I., Frise, E., Kaynig, V., Longair, M., Pietzsch, T., Preibisch, S., Rueden, C., Saalfeld, S., Schmid, B., Tinevez, J. Y., White, D. J., Hartenstein, V., Eliceiri, K., Tomancak, P., and Cardona, A. (2012) Fiji: An open-source platform for biological-image analysis. *Nat. Methods 9*, 676−682.
(67) Susaki, E. A. A., and Ueda, H. R. R. (2016) Whole-body and Whole-Organ Clearing and Imaging Techniques with Single-Cell Resolution: Toward Organism-Level Systems Biology in Mammals. *Cell Chem. Biol. 23*, 137−157.
(68) Lloyd-Lewis, B., Davis, F. M., Harris, O. B., Hitchcock, J. R., Lourenco, F. C., Pasche, M., and Watson, C. J. (2016) Imaging the mammary gland and mammary tumours in 3D: Optical tissue clearing and immunofluorescence methods. *Breast Cancer Res. 18*, 127.
(69) Boulanger, J., Kervrann, C., Bouthemy, P., Elbau, P., Sibarita, J. B., and Salamero, J. (2010) Patch-based nonlocal functional for denoising fluorescence microscopy image sequences. *IEEE Trans. Med. Imaging. 29*, 442.

https://dx.doi.org/10.1021/acsptsci.9b00090
ACS Pharmacol. Transl. Sci. 2020, 3, 63−75